Journal of Organometallic Chemistry, 394 (1990) 1–13
Elsevier Sequoia S.A., Lausanne
JOM 20538

The chemistry of monoanionic carbaborane ligands. Synthesis, and molecular and electronic structure of [3,3,3-$(CO)_3$-4-SMe_2-3,1,2-$MnC_2B_9H_{10}$], and order-of-magnitude improved structure of (η-C_5H_5)$Mn(CO)_3$ *

Jill Cowie, Ewan J.M. Hamilton, Jill C.V. Laurie ** and Alan J. Welch *
Department of Chemistry, University of Edinburgh, Edinburgh EH9 3JJ (U.K.)

(Received October 11th, 1989)

Abstract

The synthesis, and spectroscopic and structural characterisation of a transition metal complex of, formally, a monoanionic carbaborane ligand are described. Two molecules of [3,3,3-$(CO)_3$-4-SMe_2-3,1,2-$MnC_2B_9H_{10}$] crystallise in the triclinic space group $P\bar{1}$, with *a* 7.154(4), *b* 8.7890(21), *c* 13.366(3) Å, α 91.438(19), β 101.21(3), γ 110.69(3)°, at 185 ± 1 K. $R = 0.0352$ for 3859 observed reflections. The carbamanganaborane has an essentially icosahedral polyhedral geometry, and the pendant SMe_2 unit is oriented such that the S lone pair...$H(1)^{\delta+}$ interaction is maximised. The average OC–Mn–CO angle is 89.91°. A redetermination of the structure of the known species $CpMn(CO)_3$ affords molecular parameters of high precision. Space group $P2_1/a$ with *a* 11.941(7), *b* 6.981(5), *c* 10.798(7) Å, β 117.97(5)°, $Z = 4$, $R = 0.0418$ for 1960 significant reflections measured at 185 ± 1 K. In this compound OC–Mn–CO is wider, average 92.14°. Charge iterated EHMO calculations suggest that the anionic carbaborane ligand may be represented by a form in which a charge of −1.5 e on the five facial atoms is partially offset by a charge of +0.3 e on the pendant S atom. EHMO/FMO calculations confirm that the carbaborane is a better electron donor than the Cp ligand to the $\{Mn(CO)_3\}$ unit, and indicate that the additional electron density on Mn resides in fragment orbitals that are antibonding between C and O. In particular, CO → Mn σ donation is restricted in the carbaborane compound relative to the Cp compound. Consistent with the results of these calculations, ν(CO) values of the former compound are measurably lower than those of the latter species.

---

* Dedicated to Professor F.G.A. Stone on the occasion of his 65th birthday and in recognition of his many outstanding contributions to metal carbonyl chemistry and carbametallaborane chemistry.

** Present address: New Reactions Branch, B.P. Research Centre, Chertsey Road, Sunbury-on-Thames, Middx. TW 16 7LN, U.K.

Introduction

The archetypal carbaborane ligand is $[C_2B_9H_{11}]^{2-}$(carb^{2-}), first reported nearly 25 years ago and used to synthesise the first examples of carbametallaboranes [1,2]. Ever since these earliest reports an analogy has been drawn between carb^{2-} and $[C_5H_5]^-$(Cp$^-$), in that both possess 6 π electrons occupying similar frontier orbitals [3,4], and both have the ability to bond in an η^5 fashion to metal centres. To a certain extent the analogy was later refined by Hanusa [5], who argues that, in terms of its steric requirements, carb^{2-} is better compared with $[C_5Me_5]^-$(Cp$^{\star -}$).

We believe, however, that, even in its more recent version, this analogy is severely limited in its practical utility, in that it ignores the important charge difference between the two ligands. Thus we contend that species like $[(\text{carb})ML_x]^{y-}$ and $[CpML_x]^{z-}$ cannot really be compared since either (i) if M is in the same oxidation state and the ligand set L_x is common to both species, then the overall charges on the two compounds must differ by one unit ($y = z + 1$), or (ii) if the charge on the two species is to be the same, then the metal atoms must be in different oxidation states or the ligand set L_x must differ.

To date, few transition metal complexes of monoanionic carbaborane ligands have been described [6], and only a limited number of these have been fully characterised. We are interested in establishing detailed comparisons between truly analogous cyclopentadienyl- and carbaborane-metal compounds with particular emphasis on their electronic and consequent physicochemical properties. Herein we describe the synthesis, and the spectroscopic and structural characterisation of the monoanionic carbaborane-transition metal compound $[3,3,3\text{-}(CO)_3\text{-}4\text{-}SMe_2\text{-}3,1,2\text{-}MnC_2H_9H_{10}]$. For comparative purposes we have also redetermined the molecular structure of $CpMn(CO)_3$ to an accuracy an order of magnitude greater than that previously reported [7]. A comparison of the electronic structures of these two compounds has been made via the results of extended Hückel molecular orbital (EHMO) calculations.

Experimental

Syntheses

All syntheses were carried out under Schlenk line conditions, with some subsequent manipulations in the air. All solvents were dried and distilled under N_2 just before use. NMR spectra were recorded at room temperature as CD_2Cl_2 solutions on Brucker WP 80 SY (^{1}H) and WP 200 SY (^{11}B, ^{13}C) spectrometers. Infrared spectra were obtained as KBr pellets on a Perkin Elmer 598 spectrophotometer. Microanalyses were performed by the departmental service. The starting materials $9\text{-}SMe_2\text{-}7,8\text{-}C_2B_9H_{11}$ [6b], $Mn(CO)_5Br$ [8], and $[Mn(CO)_3(NCMe)_3]BPh_4$ [9] were prepared by modified versions of published methods.

Synthesis of $[3,3,3\text{-}(CO)_3\text{-}4\text{-}SMe_2\text{-}3,1,2\text{-}MnC_2B_9H_{10}]$ (1). To a mixture of finely ground KOH (0.1385 g, 2.47 mmol) and $9\text{-}SMe_2\text{-}7,8\text{-}C_2B_9H_{11}$ (0.0910 g, 0.47 mmol) in CH_2Cl_2 (10 cm^3) was added, dropwise, a suspension of $[Mn(CO)_3(NCMe)_3]BPh_4$ (0.2731 g, 0.47 mmol) in CH_2Cl_2 (15 cm^3) over a period of 20 min, during which the colour of the mixture changed from bright yellow to yellow-orange and a light-coloured flocculate precipitate separated. The mixture was stirred overnight and filtered, and the solvent removed from the filtrate in vacuo. The resulting solid was redissolved in CH_2Cl_2 (5 cm^3) and the products separated by preparative TLC (Kieselgel 60 F_{254}). Development with CH_2Cl_2 yielded **1** as a bright yellow solid (R_f 0.80, 0.047 g, 30%) (Found: C, 25.5; H, 4.72. $C_7H_{16}B_9MnO_3S$ calcd.: C, 25.3; H, 4.85%), together with a small amount of an orange, as yet unidentified, species (R_f 0.68), which by IR spectroscopy contains BH and CO functions. For **1** $\nu_{max.}$ at 2525 (B–H), 2020, 1950, and 1925 (all C–O) cm^{-1}. NMR: ^1H, δ 2.50 and 2.72 (both CH_3); ^{13}C, δ 221.9 (CO); ^{11}B, δ −0.73 (1B), −4.05 [1B, B(4)], −7.13 (1B), −7.79 (1B), −11.69 (1B), −13.07 (1B), −17.44 (1B), −19.77 (1B), and −25.23 (1B) ppm.

Synthesis of CpMn(CO)₃ (2). Tetrahydrofuran (25 cm^3) was added to a mixture of $Mn(CO)_5Br$ (1.1163 g, 4.06 mmol) and TlCp (1.0943 g, 4.06 mmol) in a foil-covered vessel, in a procedure analogous to that [10] which afforded fluorenyl- and indenyl-manganese tricarbonyl from the appropriate sodium salt. The mixture was stirred for 3 days, then filtered. The filtrate was concentrated and eluted through a Florisil column (20 × 2 cm) with CH_2Cl_2. A fast-moving yellow band was collected, from which solvent was removed in vacuo to afford a yellow solid, identified as the known species **2** by microanalysis, IR, and NMR spectroscopy.

X-Ray crystallography

All measurements were made at 185 ± 1 K with an Enraf–Nonius CAD4 diffractometer and graphite-monochromated Mo-K_α X-radiation, λ(bar) 0.71069 Å. Suitable crystals of both **1** and **2** were obtained by slow diffusion of hexane into CH_2Cl_2 solutions at −30 °C.

Compound 1. Crystal data. $C_7H_{16}B_9MnO_3S$, $M = 332.47$, triclinic, space group $P\bar{1}$, a 7.154(4), b 8.7890(21), c 13.366(3) Å, α 91.438(19), β 101.21(3), γ 110.69(3)°, V 764.5 Å^3, using 25 centered reflections, $13 < \theta < 15°$, $Z = 2$, D_c 1.444 g cm^{-3}, μ(Mo-K_α) 9.55 cm^{-1}, $F(000) = 336$.

Data collection and processing. ω–2θ scans in 96 steps, ω scan width 0.8 + 0.34 tan θ, $1 < \theta < 30°$, h 0 → 8, k −10 → 10, l −15 → 15, scan speeds 0.82–2.35° min^{-1}. 4814 data measured over ca. 128 X-ray hours, no decay or movement. 3859 reflections with $F \geq 2.0\sigma(F)$ retained.

Structure solution and refinement. Patterson synthesis for Mn position, and iterative full-matrix least-squares refinement/ΔF syntheses for all other atoms [11]. Cage C atoms identified by refined (as B) isotropic thermal parameters, and by internuclear distances. The pair of sites thus given correspond to one of two chemically sensible possibilities. Empirical absorption correction [12] applied after isotropic convergence. In the final stages all non-H atoms were refined with anisotropic thermal parameters, and all H atoms with individual isotropic parameters. Weighting scheme $w^{-1} = \sigma^2(F) + 0.000967F^2$. $R = 0.0352$, $R_w = 0.045$, $S = 1.059$. Max. and min. residues in final ΔF map 0.47 and −0.53 eÅ^{-3}. Atomic coordinates appear in Table 1. Computer programs in addition to those referenced above: CADABS [13], CALC [14], and EASYORTEP [15]. Atomic scattering factors from International Tables [16] or inlaid in SHELX76.

Compound 2. Crystal data. $C_8H_5MnO_3$, $M = 204.05$, monoclinic, space group $P2_1/a$, a 11.941(7), b 6.981(5), c 10.798(7) Å, β 117.97(5)°, V 795.0 Å^3, by the least-squares refinement of 25 centered reflections, $15 < \theta < 17°$, $Z = 4$, D_c 1.705 g cm^{-3}, μ(Mo-K_α) 15.53 cm^{-1}, $F(000) = 408$.

Data collection and processing. As for **1** except h 0 → 16, k 0 → 9, l −15 → 15,

Table 1

Fractional coordinates of atoms in 3,3,3-$(CO)_3$-4-SMe_2-3,1,2-$MnC_2B_9H_{10}$

	x	y	z
Mn(3)	0.20127(4)	0.12906(4)	0.84748(2)
S	0.27009(8)	−0.15568(5)	0.69886(4)
C(S1)	0.3293(5)	−0.1956(3)	0.57909(22)
C(S2)	0.0007(4)	−0.2671(3)	0.66932(23)
C(A)	0.2500(3)	−0.0289(3)	0.91973(16)
O(A)	0.2784(3)	−0.13069(24)	0.96441(15)
C(B)	−0.0661(3)	0.02095(25)	0.82698(16)
O(B)	−0.23858(25)	−0.04681(22)	0.81349(15)
C(C)	0.1913(4)	0.2326(3)	0.96380(19)
O(C)	0.1872(4)	0.3028(3)	1.03566(16)
C(1)	0.4903(3)	0.19644(22)	0.80137(14)
C(2)	0.4436(3)	0.35289(23)	0.83112(15)
B(4)	0.2977(3)	0.06749(23)	0.71054(15)
B(5)	0.5274(3)	0.1932(3)	0.67885(17)
B(6)	0.6241(3)	0.3783(3)	0.75971(18)
B(7)	0.2121(4)	0.3461(3)	0.76563(18)
B(8)	0.1112(3)	0.1590(3)	0.68204(17)
B(9)	0.2898(4)	0.17587(25)	0.60114(16)
B(10)	0.4916(4)	0.3695(3)	0.63164(18)
B(11)	0.4442(4)	0.4734(3)	0.73338(19)
B(12)	0.2381(4)	0.3504(3)	0.63586(18)
H(1)	0.574(4)	0.167(3)	0.8461(21)
H(2)	0.503(4)	0.409(3)	0.8949(21)
H(5)	0.624(4)	0.136(3)	0.6614(20)
H(6)	0.777(5)	0.443(4)	0.7976(25)
H(7)	0.134(5)	0.416(4)	0.7933(24)
H(8)	−0.044(4)	0.091(3)	0.6406(20)
H(9)	0.247(4)	0.115(3)	0.5245(22)
H(10)	0.564(4)	0.431(3)	0.5834(21)
H(11)	0.498(5)	0.605(4)	0.7492(24)
H(12)	0.159(5)	0.413(4)	0.5842(23)
H(S11)	0.454(7)	−0.143(5)	0.586(3)
H(S12)	0.263(5)	−0.166(4)	0.531(3)
H(S13)	0.296(5)	−0.299(4)	0.5706(23)
H(S21)	−0.047(5)	−0.268(4)	0.721(3)
H(S22)	−0.064(5)	−0.232(4)	0.617(3)
H(S23)	−0.013(5)	−0.357(4)	0.656(3)

2591 reflections measured over 60 X-ray hours, of which 1960 had $F \geq 2.0\sigma(F)$.

Structure refinement. The starting point for refinement made use of the non-H atom coordinates previously published [7]. After isotropic convergence following full-matrix least-squares refinement, empirical absorption correction applied. Thereafter all non-H atoms allowed anisotropic thermal motion. H atoms located from ΔF synthesis and all except H(8) satisfactorily refined. H(8) unstable under refinement and therefore set in fixed position. H atoms given an overall isotropic thermal parameter, 0.080(6) Å^2 at convergence. Weighting scheme $w^{-1} = \sigma^2(F) + 0.0011057F^2$. $R = 0.0418$, $R_w = 0.0600$, $S = 1.153$. Max. and min. residues in final ΔF map 0.50 and -1.06 eÅ^{-3} (near Mn). Coordinates of atoms in Table 2.

Table 2

Atomic coordinates in $(\eta\text{-}C_5H_5)Mn(CO)_3$

	x	y	z
Mn	0.28993(3)	0.00486(4)	0.26318(3)
O(1)	0.48324(18)	0.3074(3)	0.38259(24)
O(2)	0.08500(18)	0.2888(3)	0.14544(21)
O(3)	0.2672(3)	−0.0365(4)	0.52081(23)
C(1)	0.40814(21)	0.1887(3)	0.33768(25)
C(2)	0.16497(21)	0.1777(3)	0.19287(23)
C(3)	0.2757(3)	−0.0190(3)	0.4209(3)
C(4)	0.41172(25)	−0.2086(4)	0.2493(3)
C(5)	0.35952(25)	−0.0963(4)	0.1257(3)
C(6)	0.2281(3)	−0.1174(4)	0.05959(24)
C(7)	0.1977(3)	−0.2445(4)	0.1428(3)
C(8)	0.3114(3)	−0.2988(3)	0.2589(3)
H(4)	0.486(4)	−0.203(7)	0.309(5)
H(5)	0.398(5)	−0.032(6)	0.105(5)
H(6)	0.166(4)	−0.059(7)	−0.007(5)
H(7)	0.123(4)	−0.277(6)	0.129(5)
H(8)	0.333	−0.367	0.345

For both structures tables of thermal parameters and additional interbond angles and lists of observed and calculated structure factors are available from A.J.W.

Molecular orbital calculations

All calculations by a locally modified version of ICON8 [17] using the weighted H_{ij} formula [18]. To probe the preferred conformation of the SMe_2 group an idealised model of $[9\text{-}SH_2\text{-}7,8\text{-}C_2B_9H_{10}]^-$ with B–B = B–C = C–C = 1.75 Å, B–H = C–H = 1.20 Å, B–S 1.88 Å, S–H 1.28 Å, and tetrahedral angles at S was employed. H_{ii}'s used were those inlaid in ICON8. The charge iteration calculations used the crystallographically determined models of **1** and **2**. Thereafter, average H_{ii}'s (given, together with Slater exponents, in Table 3) were employed in the

Table 3

Parameters used in EHMO/FMO calculations

Orbital	H_{ii} (eV)	ζ_1	ζ_2	c_1	c_2
H(1s)	−13.30	1.30			
B(2s)	−15.40	1.30			
B(2p)	−8.68	1.30			
C(2s)	−20.90	1.625			
C(2p)	−11.10	1.625			
O(2s)	−29.10	2.275			
O(2p)	−12.50	2.275			
S(3s)	−25.10	1.817			
S(3p)	−14.50	1.817			
Mn(3d)	−11.00	5.15	1.90	0.53108	0.64788
Mn(4s)	−9.11	1.80			
Mn(4p)	−4.68	1.80			

EHMO/FMO calculations, the η-ligand models being those derived experimentally, the [$Mn(CO)_3$] units being idealised (C_{3v} symmetry, C–Mn–C 90°, Mn–C–O 180°, Mn–C 1.78 Å, C–O 1.14 Å).

Results and discussion

Synthesis, characterisation, and molecular structure of 1

The compound 9-SMe_2-7,8-$C_2B_9H_{11}$ (carb′H) [6,19] is deprotonated by an excess of KOH in CH_2Cl_2 to yield the monoanionic carbaborane ligand [9-SMe_2-7,8-$C_2B_9H_{10}$]$^-$ (carb′$^-$), which upon treatment with a convenient source of the fragment *fac*-{$Mn(CO)_3^+$} gives, after appropriate work-up, compound **1** in reasonable yield. This synthetic procedure also gives rise to a smaller amount of a second product, complete characterisation of which has so far been hampered by its relative instability.

1 has been fully identified by microanalysis and by multielement NMR spectroscopy. In the ^1H NMR spectrum there are two signals due to the S-bonded CH_3 groups, confirming their magnetic inequivalence. The ^{11}B-{^1H} NMR spectrum comprises 9 singlets all of relative integral 1. Eight of these [the exception being the 2nd highest frequency signal, at −4.05 ppm, therefore assignable to the S-bonded boron atom B(4)] display clear doublet coupling (J(BH) 138–170 Hz) on retention of proton coupling.

Thus **1** is shown to be [3,3,3-$(CO)_3$-4-SMe_2-3,1,2-$MnC_2B_9H_{10}$] [20], a rare example of a transition metal complex of a monoanionic carbaborane ligand. To establish the stereochemistry of **1**, an accurate low-temperature X-ray diffraction study was

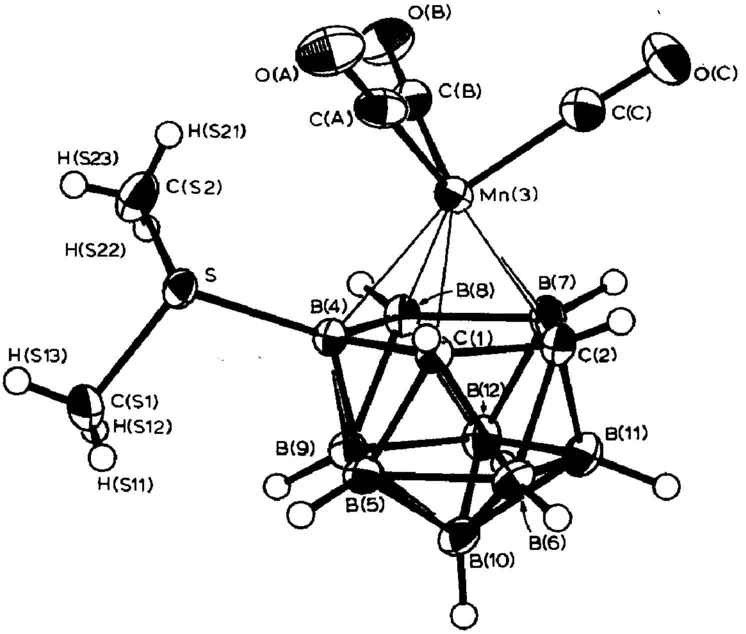

Fig. 1. Perspective view of compound **1**. All atoms drawn as 50% probability ellipsoids, except for H atoms which have an artificial radius of 0.1 Å for clarity. Cage H atoms carry the same number as the B or C to which they are bound.

Table 4

Interatomic distances (Å) and selected interbond angles (°) in 3,3,3-$(CO)_3$-4-SMe_2-3,1,2-$MnC_2B_9H_{10}$

Mn(3)–C(A)	1.8059(23)	C(2)–H(2)	0.92(3)
Mn(3)–C(B)	1.7802(22)	B(4)–B(5)	1.771(3)
Mn(3)–C(C)	1.808(3)	B(4)–B(8)	1.782(3)
Mn(3)–C(1)	2.1686(20)	B(4)–B(9)	1.768(3)
Mn(3)–C(2)	2.1688(21)	B(5)–B(6)	1.766(3)
Mn(3)–B(4)	2.1988(21)	B(5)–B(9)	1.772(3)
Mn(3)–B(7)	2.2080(25)	B(5)–B(10)	1.770(3)
Mn(3)–B(8)	2.2298(23)	B(5)–H(5)	1.05(3)
S–C(S1)	1.792(3)	B(6)–B(10)	1.775(4)
S–C(S2)	1.792(3)	B(6)–B(11)	1.761(4)
S–B(4)	1.8995(22)	B(6)–H(6)	1.06(3)
C(S1)–H(S11)	0.83(5)	B(7)–B(8)	1.797(3)
C(S1)–H(S12)	0.82(4)	B(7)–B(11)	1.791(4)
C(S1)–H(S13)	0.85(3)	B(7)–B(12)	1.780(4)
C(S2)–H(S21)	0.83(4)	B(7)–H(7)	1.07(3)
C(S2)–H(S22)	0.88(3)	B(8)–B(9)	1.805(3)
C(S2)–H(S23)	0.77(4)	B(8)–B(12)	1.797(3)
C(A)–O(A)	1.144(3)	B(8)–H(8)	1.09(3)
C(B)–O(B)	1.146(3)	B(9)–B(10)	1.777(3)
C(C)–O(C)	1.139(4)	B(9)–B(12)	1.772(3)
C(1)–C(2)	1.585(3)	B(9)–H(9)	1.08(3)
C(1)–B(4)	1.687(3)	B(10)–B(11)	1.771(4)
C(1)–B(5)	1.711(3)	B(10)–B(12)	1.783(4)
C(1)–B(6)	1.719(3)	B(10)–H(10)	0.97(3)
C(1)–H(1)	0.88(3)	B(11)–B(12)	1.764(4)
C(2)–B(6)	1.713(3)	B(11)–H(11)	1.08(3)
C(2)–B(7)	1.704(3)	B(12)–H(12)	1.09(3)
C(2)–B(11)	1.702(3)		

C(A)–Mn(3)–C(B)	90.93(10)	C(1)–B(6)–B(5)	58.77(13)
C(A)–Mn(3)–C(C)	89.92(11)	C(2)–B(6)–B(11)	58.65(13)
C(B)–Mn(3)–C(C)	88.88(11)	B(5)–B(6)–B(10)	59.99(14)
C(1)–Mn(3)–C(2)	42.88(7)	B(10)–B(6)–B(11)	60.12(14)
C(1)–Mn(3)–B(4)	45.43(7)	Mn(3)–B(7)–C(2)	65.87(11)
C(2)–Mn(3)–B(7)	45.82(8)	Mn(3)–B(7)–B(8)	66.76(11)
B(4)–Mn(3)–B(8)	47.44(8)	C(2)–B(7)–B(11)	58.20(13)
B(7)–Mn(3)–B(8)	47.76(9)	B(8)–B(7)–B(12)	60.30(13)
C(S1)–S–C(S2)	99.98(14)	B(11)–B(7)–B(12)	59.18(14)
C(S1)–S–B(4)	107.00(12)	Mn(3)–B(8)–B(4)	65.37(10)
C(S2)–S–B(4)	104.60(11)	Mn(3)–B(8)–B(7)	65.49(11)
Mn(3)–C(A)–O(A)	178.93(22)	B(4)–B(8)–B(9)	59.05(12)
Mn(3)–C(B)–O(B)	179.13(21)	B(7)–B(8)–B(12)	59.40(13)
Mn(3)–C(C)–O(C)	177.67(24)	B(9)–B(8)–B(12)	58.95(13)
Mn(3)–C(1)–C(2)	68.57(10)	B(4)–B(9)–B(5)	60.02(13)
Mn(3)–C(1)–B(4)	68.23(10)	B(4)–B(9)–B(8)	59.82(12)
C(2)–C(1)–B(6)	62.30(13)	B(5)–B(9)–B(10)	59.84(13)
B(4)–C(1)–B(5)	62.81(13)	B(8)–B(9)–B(12)	60.30(13)
B(5)–C(1)–B(6)	61.97(13)	B(10)–B(9)–B(12)	60.33(14)
Mn(3)–C(2)–C(1)	68.55(10)	B(5)–B(10)–B(6)	59.74(13)
Mn(3)–C(2)–B(7)	68.30(11)	B(5)–B(10)–B(9)	59.95(13)
C(1)–C(2)–B(6)	62.69(13)	B(6)–B(10)–B(11)	59.54(14)
B(6)–C(2)–B(11)	62.07(14)	B(7)–B(10)–B(12)	60.10(14)
B(7)–C(2)–B(11)	63.46(14)	B(9)–B(10)–B(12)	59.70(14)
Mn(3)–B(4)–C(1)	66.33(10)	B(11)–B(10)–B(12)	59.49(14)
Mn(3)–B(4)–B(8)	67.19(10)	C(2)–B(11)–B(6)	59.28(13)

Table 4 (continued)

C(1)-B(4)-B(5)	59.25(12)	C(2)-B(11)-B(7)	58.34(13)
B(5)-B(4)-B(9)	60.12(13)	B(6)-B(11)-B(10)	60.35(14)
B(8)-B(4)-B(9)	61.13(13)	B(10)-B(11)-B(12)	60.59(14)
C(1)-B(5)-B(4)	57.93(12)	B(7)-B(12)-B(8)	60.29(13)
C(1)-B(5)-B(6)	59.26(13)	B(7)-B(12)-B(11)	60.72(14)
B(4)-B(5)-B(9)	59.86(13)	B(8)-B(12)-B(9)	60.76(13)
B(6)-B(5)-B(10)	60.27(14)	B(9)-B(12)-B(10)	59.97(14)
B(9)-B(5)-B(10)	60.21(13)	B(10)-B(12)-B(11)	59.91(14)
C(1)-B(6)-C(2)	55.01(12)		

undertaken, and afforded highly precise structural parameters. Figure 1 shows a perspective view of **1** and the atomic numbering scheme used. Table 4 lists the interatomic distances and selected interbond angles.

Clearly, the geometry of the polyhedron of **1** is that of a closed icosahedron. The manganese atom is 1.643 Å from the best (least-squares) plane through the C(1)C(2)B(4)B(7)B(8) face, which is slightly folded into an envelope conformation. Usually for icosahedral 1,2-dicarba-3-metallaboranes [21] the fold is along the C(2)...B(8) vector, and is such that the 3 and 4 atom portions (defined by C(2)B(7)B(8) and C(2)C(1)B(4)B(8) respectively) are bent towards the metal, affording fold parameters [21] ϕ −2.40°, θ −1.52°. The manganese atom is somewhat closer to C(1) and C(2) than to the facial boron atoms, but this merely reflects the smaller polyhedral radius of C than of B, since calculation reveals no slip of Mn(3) relative to the lower pentagonal belt [B(5)B(6)B(11)B(12)B(9)].

The $\{Mn(CO)_3\}$ fragment is oriented with respect to the carb′ ligand such that one carbonyl function, C(B)O(B), is essentially trans to the mid-point of the C(1)-C(2) connectivity (see Fig. 2, a view of **1** from a position above the manganese atom). The Mn–C(B) bond is significantly shorter than the other two. This *trans* influence of the cage carbon atoms is readily understood in terms of the fact that the frontier orbitals of *nido*-C_2B_9 ligands have been shown to be localized predominantly on the facial boron atoms [4]. Surprisingly, no similar *trans* influence is

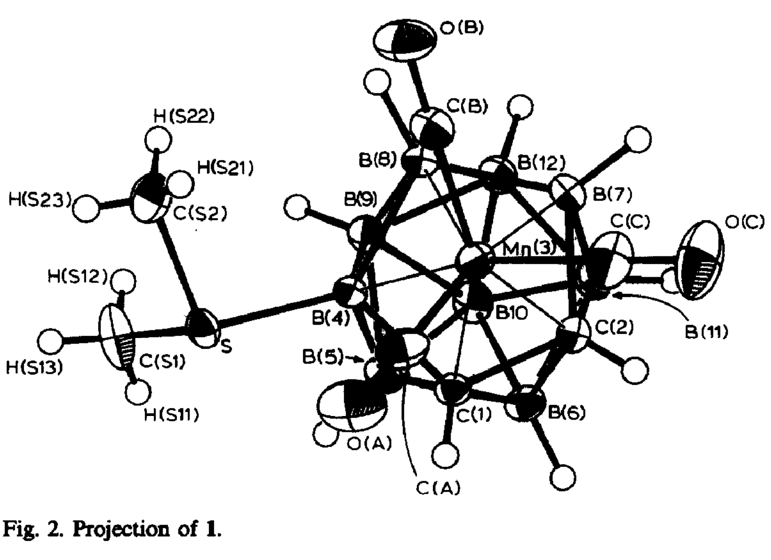

Fig. 2. Projection of 1.

observed in the related complex $[(\mathrm{carb})\mathrm{Re}(\mathrm{CO})_3]^-$ [22]. Since, in **1**, Mn–C(A) = Mn–C(C) there appears to be no perceptible difference in *trans* influence between the {B(4)SMe$_2$} unit and the {B(7)H} function.

The orientation of the SMe$_2$ unit is of some interest. As Figure 2 clearly shows, the torsion about the B(4)–S bond is such that the sulphur lone pair nearly eclipses the B(4)–C(1) connectivity (the torsion angle C(1)–B(4)–S-lone pair, calculated from the measurable angles C(1)–B(4)–S–C(S1) and C(1)–B(4)–S–C(S2) is only 4.1(3)°). Moreover, the angle C(1)–B(4)–S, 117.82(13)°, is substantially narrower than B(8)–B(4)–S, 130.47(14)°, i.e. the sulphur lone pair is inclined towards C(1)H(1). Since there is no evidence of intramolecular crowding involving the methyl groups and cage H atoms ($\mathrm{H}_{\mathrm{methyl}} \cdots \mathrm{H}_{\mathrm{cage}} > 2.40$Å), and since it is well known [23] that the H atoms terminal to carbaborane C atoms are relatively protonic, we suggest that the preferred orientation of the SMe$_2$ unit is that which maximises the lone pair... $\mathrm{H}(1)^{\delta+}$ interaction. Consistent with this, EHMO calculations using an idealised model of $[9\text{-SH}_2\text{-}7,8\text{-C}_2\mathrm{B}_9\mathrm{H}_{10}]^-$ reveal that the optimum energy is reached when the C(7)–B(9)–S-lone pair [20] torsion angle is exactly 0°. Similar torsions and inclinations of the SMe$_2$ group are observed in the structure of carb′H itself [19] and in the isolobally-substituted species 10,11-μ-(Ph$_3$P)Au-9-SMe$_2$-7,8-C$_2$B$_9$H$_{10}$ [24], presumably for the same reason as that discussed above for **1**.

Molecular structure of 2

An early crystallographic study of **2** was reported previously [7], but by today's standards it was of low precision. Therefore, to enable meaningful comparison between **1** and **2** to be made, we redetermined the solid state structure of **2**, and achieved a final model which, in terms of estimated standard deviations, is an order of magnitude better than that previously reported. Interatomic distances and selected interbond angles are given in Table 5.

Table 5

Interatomic distances (Å) and selected interbond angles (°) in (η-C$_5$H$_5$)Mn(CO)$_3$

Mn–C(1)	1.7947(25)	O(3)–C(3)	1.137(4)
Mn–C(2)	1.7876(25)	C(4)–C(5)	1.416(4)
Mn–C(3)	1.797(3)	C(4)–C(8)	1.399(4)
Mn–C(4)	2.136(3)	C(4)–H(4)	0.81(5)
Mn–C(5)	2.133(3)	C(5)–C(6)	1.394(4)
Mn–C(6)	2.141(3)	C(5)–H(5)	0.75(6)
Mn–C(7)	2.142(3)	C(6)–C(7)	1.426(4)
Mn–C(8)	2.139(3)	C(6)–H(6)	0.85(5)
O(1)–C(1)	1.148(3)	C(7)–C(8)	1.401(4)
O(2)–C(2)	1.148(3)	C(7)–H(7)	0.86(5)
C(1)–Mn–C(2)	91.85(11)	Mn–C(1)–O(1)	178.58(24)
C(1)–Mn–C(3)	92.63(12)	Mn–C(2)–O(2)	178.68(23)
C(2)–Mn–C(3)	91.94(12)	Mn–C(3)–O(3)	179.1(3)
C(4)–Mn–C(5)	38.74(11)	C(5)–C(4)–C(8)	107.8(3)
C(4)–Mn–C(8)	38.21(11)	C(4)–C(5)–C(6)	108.46(25)
C(5)–Mn–C(6)	38.07(11)	C(5)–C(6)–C(7)	107.5(3)
C(6)–Mn–C(7)	38.89(11)	C(6)–C(7)–C(8)	107.8(3)
C(7)–Mn–C(8)	38.20(12)	C(4)–C(8)–C(7)	108.5(3)

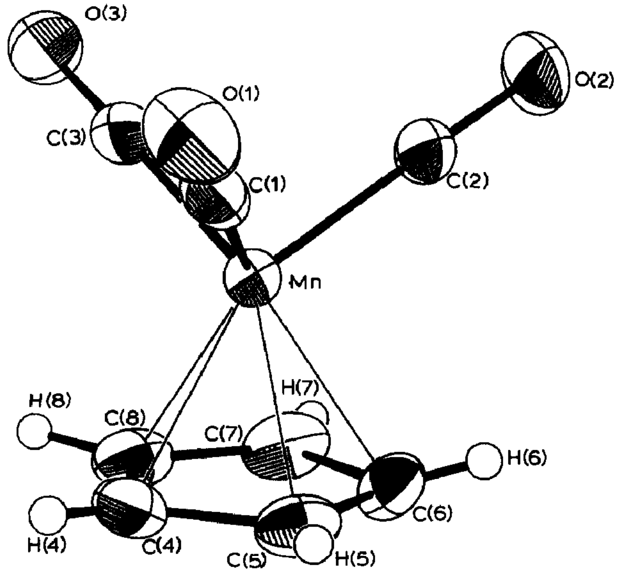

Fig. 3. Perspective view of compound **2**. Thermal ellipsoids as for Fig. 1.

The molecule, which is viewed in perspective and in projection in Fig. 3 and 4, respectively, has effective C_s point group symmetry about the plane defined by Mn, C(1), O(1), and C(7). That carbonyl carbon atom [C(2)] which is most trans to a C–C(Cp) edge is significantly closer to Mn than are the other two, but there is no significant variation in C–O distances. The manganese atom is 1.772 Å from the C_5 plane and all the H atoms are slightly (3–9°) inclined out of this plane towards Mn. In **1** the Mn–η-plane distance is less because the ligand face is larger [25].

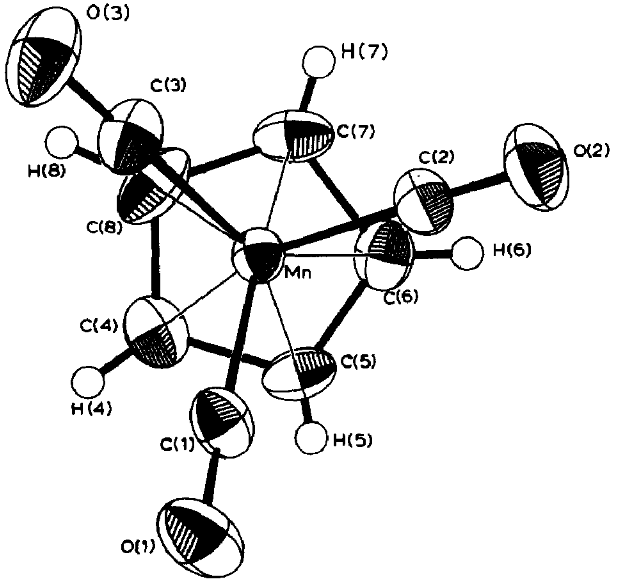

Fig. 4. Projection of **2**.

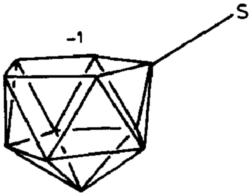

I

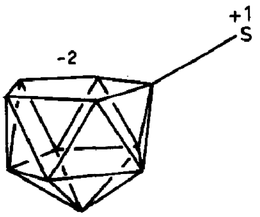

II

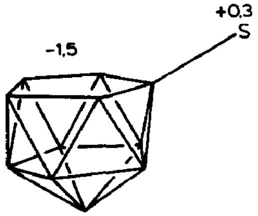

III

Comparison of the molecular and electronic structures of 1 and 2

The [carb′]$^-$ ligand may be drawn in two extreme forms. In I there is a net charge of −1 located on the atoms of the pentagonal face, whereas in the zwitterionic form II the net charge on the facial atoms is −2.

In an attempt to assess the relevance of these alternate forms of [carb]$^-$ in complex **1** we performed EHMO calculations on the crystallographically derived models of both **1** and **2** with full charge iteration on all atoms. These calculations reveal that in **1** the $\{Mn(CO)_3\}$ fragment carries a total charge of −0.51 e, i.e. 1.51 e is transferred from the carbaborane ligand to an $\{Mn(CO)_3^+\}$ unit. In contrast, the $\{Mn(CO)_3\}$ fragment in **2** has a total charge of only −0.20 e.

Thus, the carb′ ligand in **1** is a significantly better electron donor than is the Cp ligand in **2**. Clearly this difference is related to the fact that the occupied frontier orbitals of the carbaborane ligand contain substantial amounts of B $2p$ character, and are therefore higher lying than the corresponding orbitals of Cp. Although carbaborane ligands are often regarded as the archetypal electron deficient ligands they are, of course, electron precise for the structures they adopt, and the above results are certainly sensible in terms of the difference in size of the 5 atom ligand faces of carb′ and Cp and the difference in H_{ii}'s of the atoms that define those 5 atom faces. The calculations show that carb′ transfers 0.31 e more to the metal centre than does Cp. Given that the S atom in **1** is calculated to carry a charge of +0.26 e, the results suggest that a reasonable description of the electron partitioning in the anionic carbaborane ligand is that given in III.

Part of the reason for selecting compounds **1** and **2** for comparison resided in the potential of the carbonyl ligands common to both species to reflect the amount of charge transfer between the anionic ligands and the metal atom. The crystallographic results show that there is no measurable difference in either Mn–C or C–O bond distances between **1** and **2**, implying that any differences in bonding within the $\{Mn(CO)_3\}$ moiety are small. The charge iterated EHMO calculations indicate that the metal tricarbonyl unit in **1** is somewhat more negative than that in **2**. Subsequent EHMO/FMO calculations (using models of **1** and **2** built up of crystallographically determined η-ligands (carb′ or Cp) and idealised $\{Mn(CO)_3\}$ units positioned and oriented over the η-ligand face as found in the crystal structures, and using the averaged optimised H_{ii}'s given in Table 3) show that 80% of the extra charge on the metal resides in the e acceptor orbitals (LUMO) of $\{Mn(CO)_3^+\}$, 20% in the a_1 acceptor orbital (2nd LUMO) [25] (Fig. 5). Build up of charge in these e orbitals limits σ donation from carbonyl ligand to metal, and since the HOMO of CO is antibonding between C and O, prevents the C–O bond from strengthening.

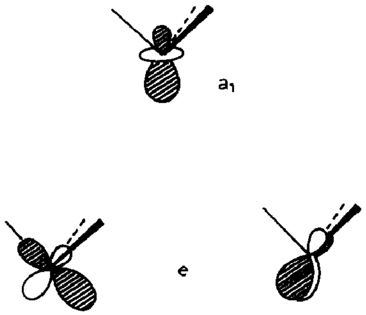

Fig. 5. The *e* and a_1 acceptor orbitals of $\{Mn(CO)_3^+\}$.

At the same time the slight additional charge in the a_1 acceptor orbital of the $\{Mn(CO)_3^+\}$ fragment in **1** versus **2** is in an orbital of the correct symmetry for interaction with the C–O π^* system. Both these features suggest that the C–O bonds in **1** should be somewhat weaker than those in **2**. Indeed, the EHMO/FMO calculations give C–O bond overlap populations of 1.278–1.292 for the carb′ compound **1** and 1.295–1.296 for the Cp compound **2**.

In agreement with these theoretical conclusions, the C–O stretching frequencies [26,27] of **1** are slightly lower than those of **2**, by an average of 7 cm^{-1}. On its own, a result like this would generally be held to be of little significance, and certainly the difference is a small one. It is, however, fully consistent with the greater donor ability of carb′ versus Cp, and it correlates perfectly with the C–O bond overlap populations calculated above, so we are confident that it is a meaningful result. It is equally satisfying that our accurate redetermination of the structure of **2** affords an average OC–Mn–CO bond angle of 92.14° (c.f. 89.91° in **1**) which fits perfectly with the prediction of Haas and Sheline [27] that the angle in **2** would be obtuse on the basis of the relative integrated absorption coefficients of the *e* and *a* vibrations.

Acknowledgements

We thank the SERC (EJMH) and SED (JC) for support.

References

1 M.F. Hawthorne, D.C. Young, and P.A. Wegner, J. Am. Chem. Soc., 87 (1965) 1818.
2 M.F. Hawthorne, D.C. Young, T.D. Andrews, D.V. Howe, R.L. Pilling, A.D. Pitts, M. Reintjes, L.F. Warren Jnr., and P.A. Wegner, J. Am. Chem. Soc., 90 (1968) 879.
3 W.L. Jørgenson and L. Salem, The Organic Chemist's Book of Orbitals, Academic Press, New York, 1973.
4 D.M.P. Mingos, J. Chem. Soc., Dalton Trans., (1977) 602.
5 T.P. Hanusa, Polyhedron, 1 (1982) 663.
6 For example: (a) M.F. Hawthorne, L.F. Warren Jr., K.P. Callahan, and N.F. Travers, J. Am. Chem. Soc., 93 (1971) 2407; (b) J. Plesek, Z. Janousek, and S. Hermanek, Collect. Czech. Chem. Commun., 43 (1978) 2862; (c) R.G. Teller, J.J. Wilczyynski, and M.F. Hawthorne, J. Chem., Soc., Chem. Commun., (1979) 472.
7 A.F. Berndt and R.E. Marsh, Acta Crystallogr., 16 (1963) 118.
8 M.H. Quick and R.J. Angelici, Inorg. Synth., 19 (1980) 160.
9 R.H. Reimann and E. Singleton, J. Chem. Soc., Dalton Trans., (1974) 808.
10 R.B. King and A. Efraty, J. Organomet. Chem., 23 (1970) 527.

11 SHELX76; G.M. Sheldrick, University of Cambridge, 1976.
12 DIFABS; N.G. Walker and D. Stuart, Acta Crystallogr., A, 39 (1983) 158.
13 CADABS; R.O. Gould and D.E. Smith, University of Edinburgh, 1986.
14 CALC; R.O. Gould and P. Taylor, University of Edinburgh, 1986.
15 EASYORTEP; P.D. Mallinson and K.W. Muir, J. Appl. Cryst., 18 (1985) 51.
16 International Tables for X-Ray Crystallography, Kynoch Press, Birmingham, Vol. 4, 1974, p. 99.
17 ICON8; J. Howell, A. Rossi, D. Wallace, K. Haraki, and R. Hoffmann, Quantum Chemistry Program Exchange, University of Indiana, no. 344.
18 J.H. Ammeter, H.-B. Burgi, J.C. Thibeault, and R. Hoffmann, J. Am. Chem. Soc., 100 (1982) 3686.
19 J. Cowie, E.J.M. Hamilton, J.C.V. Laurie, and A.J. Welch, Acta Crystallogr., C, 44 (1988) 1648.
20 Unfortunately, conventional nomenclature (J.B. Casey, W.J. Evans, and W.H. Powell, Inorg. Chem., 22 (1983) 2228; 2236) dictates that the heteroatom numbering in ligand and its transition metal complex are different.
21 D.M.P. Mingos, M.I. Forsyth, and A.J. Welch, J. Chem. Soc., Dalton Trans., (1978) 1363; D.E. Smith and A.J. Welch, Organometallics, 5 (1986) 760; D.E. Smith and A.J. Welch, Acta Crystallogr., C, 42 (1986) 1717.
22 A. Zalkin, T.E. Hopkins, and D.H. Templeton, Inorg. Chem., 5 (1966) 1189.
23 R.N. Grimes, Carboranes, Academic Press, New York, 1970, p. 66.
24 E.J.M. Hamilton and A.J. Welch, Acta Crystallogr., C, in press.
25 M. Elian, M.M.L. Chen, D.M.P. Mingos, and R. Hoffmann, Inorg. Chem., 15 (1976) 1148.
26 T.S. Piper, F.A. Cotton, and G. Wilkinson, J. Inorg. Nucl. Chem., 1 (1955) 165.
27 H. Hass and R.K. Sheline, J. Chem. Phys., 47 (1967) 2996.